For presentation at the 11th annual conference of the Canadian Applied Mathematics Society, Halifax 29 May - 1 June 1990

Numerical simulation of nonlinear wave groups

W.M. Drennan†, J.D. Fenton‡and M.A. Donelan†

†National Water Research Institute, Canada Centre for Inland Waters, P. O. Box 5050, Burlington, Ontario L7R 4A6

‡Department of Civil Engineering, University of Auckland, Private Bag, Auckland, New Zealand

Abstract

The Fourier wave method, based on collocation theory, is employed to study the evolution of nonlinear wave groups in a wave tank. The flow is assumed to be two dimensional and irrotational, and the tank is discretized into evenly spaced points along its length. The spatial variation of the velocity potential and free surface, at a given time, are approximated by truncated Fourier series, with evolution in time achieved using a second order finite difference scheme.

This work was carried out to complement that of Pierson, Donelan and Hui who carried out a series of experiments investigating the linear and nonlinear propagation of wave groups down a tank. With our numerical model, we look at the dispersion and coalescence of wave groups such as the Gaussian wave packet. The differences between linear and nonlinear propagation will be discussed.

1. Introduction and Formulation

We consider the problem of the two dimensional, irrotational evolution of nonlinear wave groups travelling through an incompressible, inviscid fluid in a region Ω, a wave tank bounded by a horizontal plane bottom of length L, vertical plane sides and the interface between the water and air. We employ a Cartesian coordinate system (x, y) centred at a bottom corner of the tank with x in the horizontal direction and y pointing upwards. The water surface is denoted $y = \eta(x, t)$. For convenience, we employ dimensionless variables in which length scales are multiplied by π/L, time (t) by $\sqrt{g\pi/L}$, where g is the gravitational constant, and the velocity potential (ϕ) by $\sqrt{(\pi/L)^3/g}$. Under the above assumptions, the fluid motion in Ω is governed by

$$\nabla^2\phi = 0 \tag{1}$$

$$\phi_y = 0 \text{ on } y = 0 \tag{2}$$

$$\phi_x = 0 \text{ on } x = 0, \pi \tag{3}$$

$$\eta_t + \phi_x\eta_x - \phi_y = 0 \text{ on } y = \eta(x,t) \tag{4}$$

$$\phi_t + \frac{1}{2}(\phi_x^2 + \phi_y^2) + \eta = 0 \text{ on } y = \eta(x,t) \tag{5}$$

$$\eta(x,0) = f(x) \tag{6}$$

$$\eta_t(x,0) = g(x) \tag{7}$$

where the subscripts denote partial differentiation.

Due to the complexity of the above system, which is nonlinear and involves a free boundary, analytic solutions have, to date, proven to be elusive. The choice of an appropriate coordinate transform, such as the pressure formulation of Hui and Tenti [1] offers some hope for future progress, but at present, the resulting algebra is prohibitive. With the paucity of analytic results, many researchers have employed numerical schemes to investigate the problem. Noteworthy among these are Longuet-Higgins and Cokelet [2] and Dold and Peregrine [3] who, using boundary integral techniques, have been able to follow the evolution of a plunging wave almost to the point of breaking. Such techniques, however, are complicated to implement. For flows in which the wave surface, $\eta(x,t)$ remains single valued, there exists an alternative approach which is both accurate and relatively simple.

2. The Fourier method

The Fourier or pseudospectral method employs truncated Fourier series to approximate horizontal (spatial) variation with a finite difference scheme for temporal variation. The method was proposed by Orszag [4] and has subsequently been employed by Fornberg and Whitham [5] in a study of the Korteweg-de Vries equation and Fenton and Rienecker [6] in their investigations of solitary wave interaction. Abe and Inoue [7] compared numerical solutions of the KdV equation, found via Fourier and finite difference methods, and concluded that the former method was both more accurate and more effective. A useful summary of recent work applying the Fourier method to the steady wave problem can be found in Sobey [8]. We note here that the foundations of the theory are to be found in the collocation method of finite elements, with the truncated set of trigonometric functions forming the set of basis functions.

In Fourier wave theory, it is assumed that ϕ and η are periodic in the x-direction with wavelength 2π ($2L$ in dimensional coordinates). We can then write

$$\phi(x,y,t) = \sum_{j=0}^{N-1} A_j(t) \frac{\cosh jy}{\cosh jd} \cos jx \tag{8}$$

where N the order of truncation and d is the average depth. (The deep water case is handled by shifting the coordinate axis to the mean water level and replacing the hyperbolic function with exponentials.) This form satisfies Laplace's equation (1) as well as the bottom (2) and end wall (3) boundary conditions. The N coefficients $A_j(t)$ are found at each point in time by satisfying the kinematic (4) and dynamic (5) boundary conditions at N discrete points ($x_m = \frac{m\pi}{N-1}, m = 0, \ldots, N-1$) of the free surface; the N free surface values $\eta(x_m,t)$ are found at the same time. One advantage of the Fourier method is that the spatial derivatives are easily calculated from the original Fourier series. From the series for η,

$$\eta(x_m,t) = \eta_m = \sum_{j=0}^{N-1} B_j(t) \cos jx_m, \tag{9}$$

the discrete Fourier transform yields

$$B_j(t) = \mathcal{F}(\eta) = \frac{2}{N-1} \sum_{n=0}^{N-1} \eta_n \cos(\frac{jn\pi}{N-1}). \tag{10}$$

The spatial derivative of η is then given by

$$\frac{\partial \eta}{\partial x}(x_m, t) = -\sum_{j=0}^{N-1} jB_j(t) \sin jx_m, \tag{11}$$

— i.e. the inverse Fourier transform of (jB_j). We note here that the accuracy of this step, and indeed of the method itself, relies on the capability to approximate the unknown functions ϕ and η by *truncated* Fourier series. If the functions are sufficiently smooth (nonsharp), the Fourier coefficients will decay with increasing frequency at an almost exponential rate, and the approximation will be an excellent one. If, however, there is a slope discontinuity, as with a sharp crest, the coefficients will decay slowly and a large number of them will be required to adequately represent the function — in this case truncation may result is errors which will rapidly render the solution useless. In practice, the magnitude of N and therefore the steepness of waves which can be approximated using Fourier theory is limited by the available computer memory.

In order to advance the solution in time, a second order finite difference scheme is employed. In particular, we use

$$\eta(x_m, t+\Delta) = \eta(x_m, t-\Delta) + 2\Delta \frac{\partial \eta}{\partial t}(x_m, t) + O(\Delta^3) \tag{12}$$

where Δ denotes the time step. Note that in order to advance the solution in time, we require initial values at times 0 and Δ. Given η and η_t at time 0 (by (6) and (7)), we calculate the A_j's from (4) by solving a linear system of equations. We then solve for η and the A_j's at time Δ using a first order finite difference scheme with ten steps of $\Delta/10$. Then, given solution vectors A and η at two times t and $t-\Delta$, the calculation of $A_j(t+\Delta)$ and $\eta(x_m, t+\Delta)$ proceeds as follows: at time t,

$$\begin{aligned}
\text{calculate} \quad & \phi_x = -\sum_{j=0}^{N-1} jA_j \frac{\cosh j\eta_m}{\cosh jd} \sin jx_m \\
& \phi_y = \sum_{j=0}^{N-1} jA_j \frac{\sinh j\eta_m}{\cosh jd} \cos jx_m \\
& \phi_t = -\eta - \frac{1}{2}(\phi_x^2 + \phi_y^2), \\
\text{solve } N \text{ x } N \text{ system} \quad & \phi_t = \sum_{j=0}^{N-1} \frac{dA_j}{dt} \frac{\cosh j\eta_m}{\cosh jd} \cos jx_m \quad \text{for } \frac{dA_j}{dt}, \\
\text{calculate} \quad & \eta_x = i\mathcal{F}^{-1}(j\mathcal{F}(\eta)) \\
& \eta_t = \phi_y - \phi_x \eta_x, \\
\text{and finally} \quad & A_j(t+\Delta) = A_j(t-\Delta) + 2\Delta \frac{dA_j}{dt}(t) \\
& \eta(x_m, t+\Delta) = \eta(x_m, t-\Delta) + 2\Delta \frac{\partial \eta}{\partial t}(x_m, t).
\end{aligned}$$

In summary, we note that the Fourier method requires two independent approximations. The first is that the Fourier series be truncated — this was discussed above. The second is the finite difference approximation to the time derivative. This latter error can be controlled to some degree through the choice of Δ, at the expense of increased computational time. A linear stability analysis for the scheme has been carried out by Fenton and Rienecker [6] with the result that $\Delta \leq (N-1)^{-1/2}$. This yields an upper bound on the largest time step which can be employed at a given truncation order. As a check on the accuracy of the solution, the conservation of total energy requirement was strictly enforced. A sudden change in energy at some time step was a sign that stability was lost in the solution — this was typically corrected by decreasing the time step.

3. Numerical results

We choose as our initial conditions the Gaussian wave packet given by

$$\eta(x) = -\frac{A}{D^{1/4}} e^{-\frac{16x^2B^2}{T^2g^2D}(x-gTt/4\pi)^2} \sin\left(\frac{4\pi^2 x}{DgT^2} - \frac{2\pi t}{DT} - \frac{4B^4t^2x}{Dg} + \frac{1}{2}\arctan 4B^2x/g\right) \qquad (13)$$

where $D = 1 + 16B^4x^2/g^2$. In a recent set of experiments conducted in the National Water Research Institute's 100 metre wave tank by Pierson, Donelan and Hui [9], low amplitude Gaussian wave packets were produced at the wave board and allowed to propagate linearly down the tank past a wave gauge where their passage was recorded. The dispersed wave trains were then reversed, amplified and fed as input signals to the wave board. We have simulated the resulting nonlinear coalescence by starting with a reversed wave packet (13).

The algorithm was coded in Matlab and run on an Everex 386-20 computer. With N=256, each time step took approximately one minute; at N=128, this was considerably reduced. As a sample of our output, we present two runs for the case $A = 0.15$ with $N = 256$, $B = 1/\sqrt{3}\text{s}^{-1}$, $T = 1.5$s and $t = 27.52$s in (13). Figures 1–3 illustrate wave evolution according to linear theory, in which all nonlinear terms have been dropped from the algorithm. We have followed the solution for 2100 time steps of size $\Delta = 0.01$. During this time, the wave form (Figure 1) can be seen to coalesce (a–c), reflect from the tank wall (d) and disperse (e). Figure 2 illustrates the time series of the wave signal as it passes three points in the tank. Note the passing of the initial train and then that of the reflected signal. At the third station, near the end wall, the two signals interfere with each other to some degree. In Figure 3, the total, kinetic and potential energies are displayed. Note that equipartition of energy holds until the wave signal reaches the wall at which point standing wave effects are evident.

In Figure 4(a) we examine the changes in the time series at the point $x = 198\pi/255$ when the full nonlinear solution is implemented. There is a small but noticeable advance in the phase of the nonlinear solution over the linear, implying an increase in the phase propagation speed. The envelopes corresponding to Figure 4(a) are displayed in Figure 4(b), wherein the increase in propagation speed of the envelope maximum is apparent. This numerical method offers an

interesting opportunity to study the behaviour of envelope soliton solutions of the nonlinear (third order) Schrödinger equation. The existence of envelope solitons hinges on the delicate balance between frequency and amplitude dispersion leading to an increase in the envelope propagation speed, which we see here at relatively modest steepnesses.

Finally, we demonstrate the rapid spectral changes that arise through the nonlinear interactions among the components that make up the packet. For comparison, the spectral densities computed from the solution at several stages in the evolution are shown for the linear solution (Figure 5(a)) and nonlinear solution (Figure 5(b)). In both cases, the envelope coalesces to the point of maximum steepness and continues beyond this point to disperse again as the longer (faster) wave components move through the group and emerge at the front. In the linear case, the spectra remain unchanged, as expected. By contrast, the nonlinear case shows pronounced spreading of the energy from the region of the peak to higher and lower frequencies. When the point of maximum coalescence has passed the spectrum changes less rapidly, but shows no tendency to revert to its earlier state — the process is irreversible.

References

1. Hui, W. and Tenti, G. "Nonlinear wave theory via pressure formulation" in "The ocean surface" (Eds. Toba, Y. and Mitsuyasu, H.), Reidel, Dordrecht, 17-24, 1985.
2. Longuet-Higgins, M. and Cokelet, E. "The deformation of steep surface waves on water I. A numerical method of computation", Proc. R. Soc. London A350, 1-26, 1976.
3. Dold, J. and Peregrine, D. "Steep unsteady water waves : an efficient computational scheme", in Proc. 19th Int. Conf. on Coastal Eng., Houston, 955-967, 1984.
4. Orszag, S. "Numerical simulation of incompressible flows within simple boundaries. I. Galerkin (spectral) representations", Stud. in App. Math. 50, 293-327, 1971.
5. Fornberg, B. and Whitham, G. "A numerical and theoretical study of certain nonlinear wave phenomena", Phil. Trans. R. Soc. London A289, 373-404, 1978.
6. Fenton, J. and Rienecker M. "A Fourier method for solving nonlinear water-wave problems: application to solitary wave interactions", J. Fluid Mech. 118, 411-443, 1982.
7. Abe, K. and Inoue, O. "Fourier expansion solution of the Korteweg-de Vries equation", J. Comput. Phys 34, 202-210, 1980.
8. Sobey, R. "Variations on Fourier wave theory", Int. J. Num. Meth. Fluids 9, 1453-1467, 1989.
9. Pierson, W. Jr., Donelan, M. and Hui, W. "Linear and nonlinear propagation of water wave groups", (manuscript in preparation).

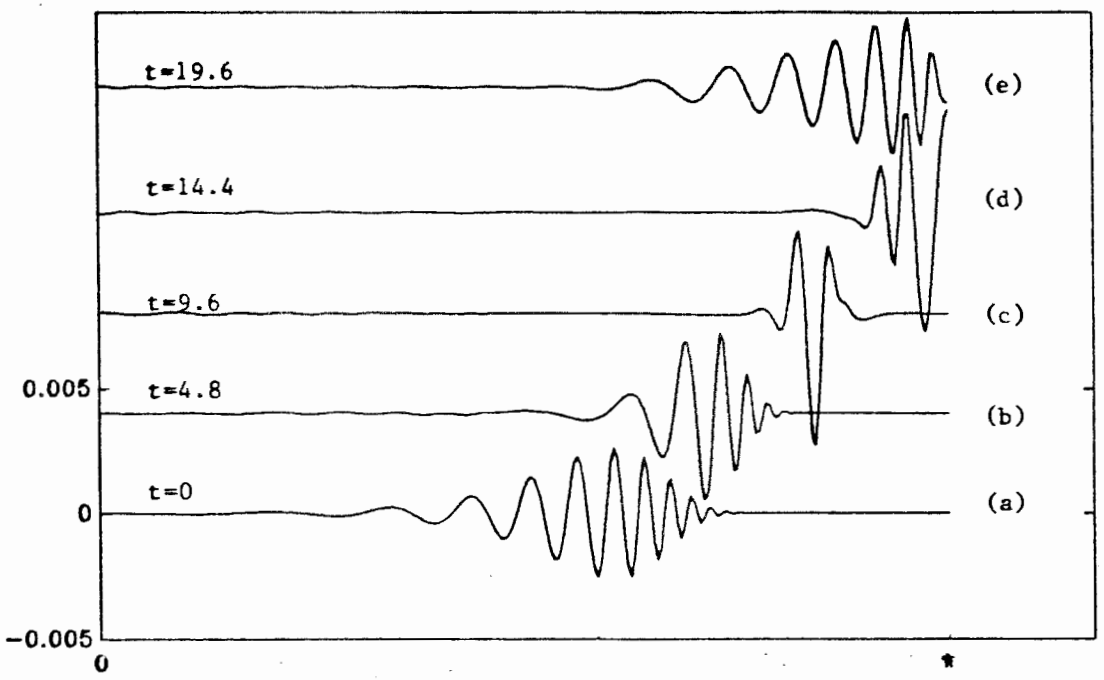

FIG.1 Evolution of linear wave form: space series

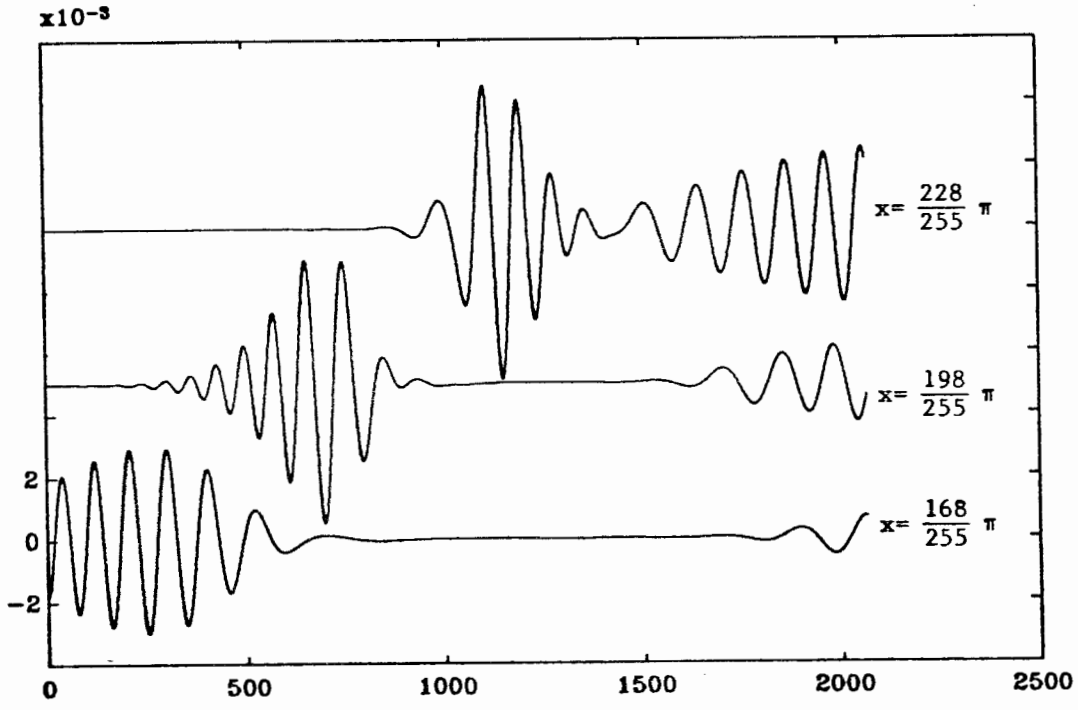

FIG.2. Three time series (linear theory, A=0.15)

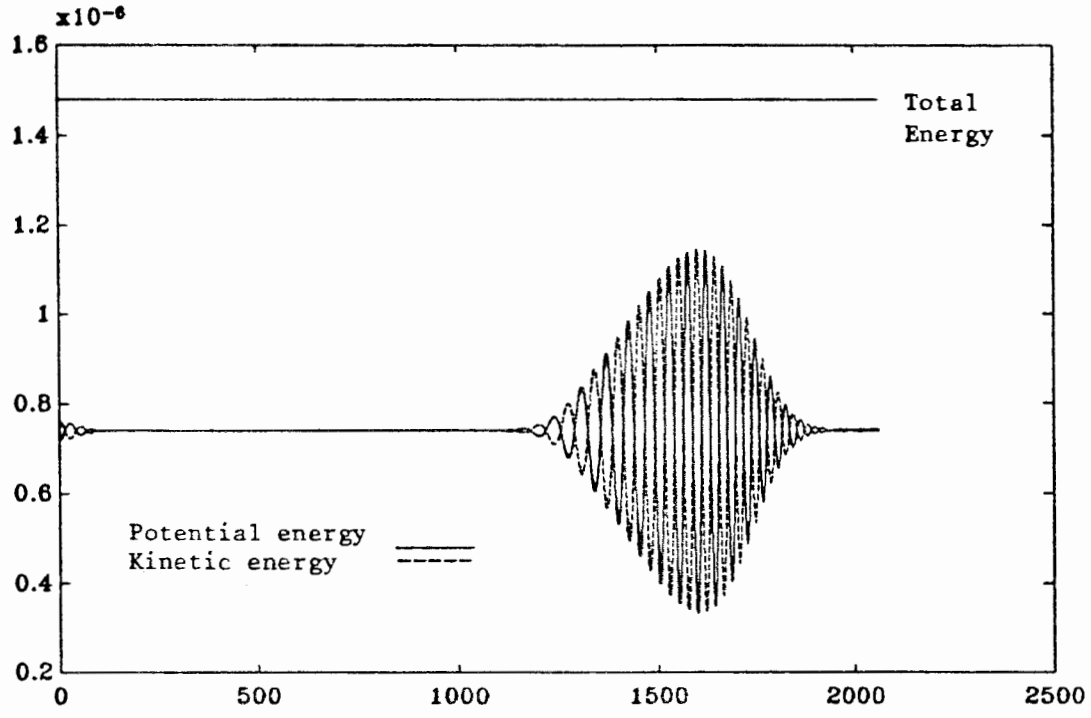

FIG. 3. Energy vs time (linear theory, A=0.15)

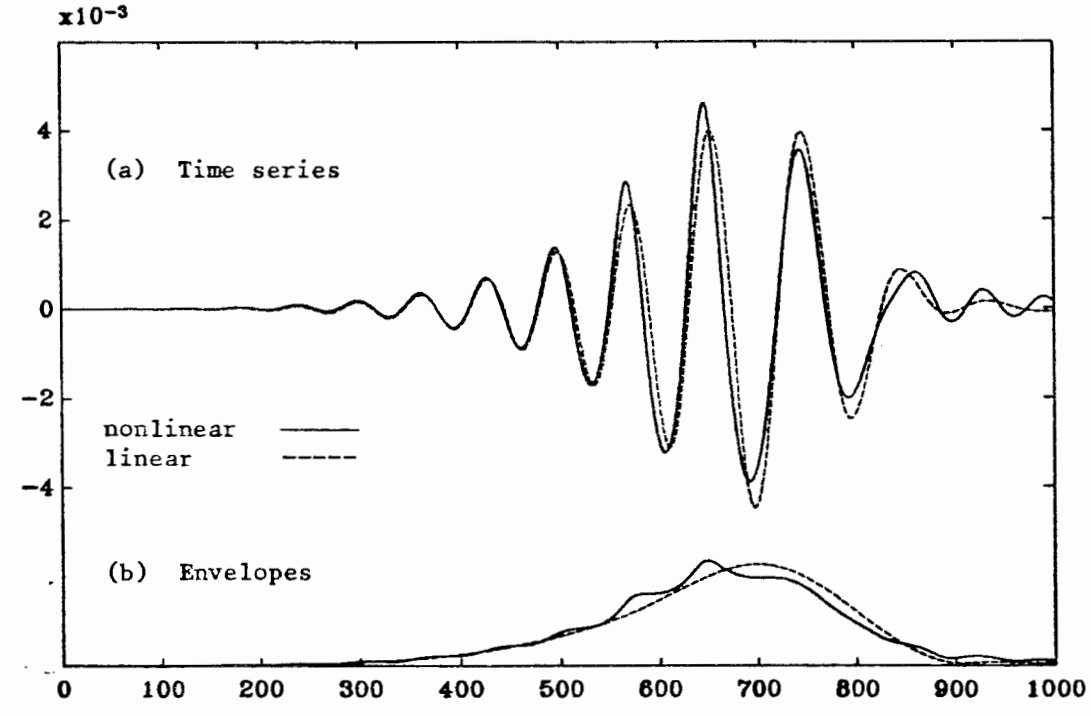

FIG. 4. Nonlinear and linear time series at $x = \frac{198}{255}\pi$

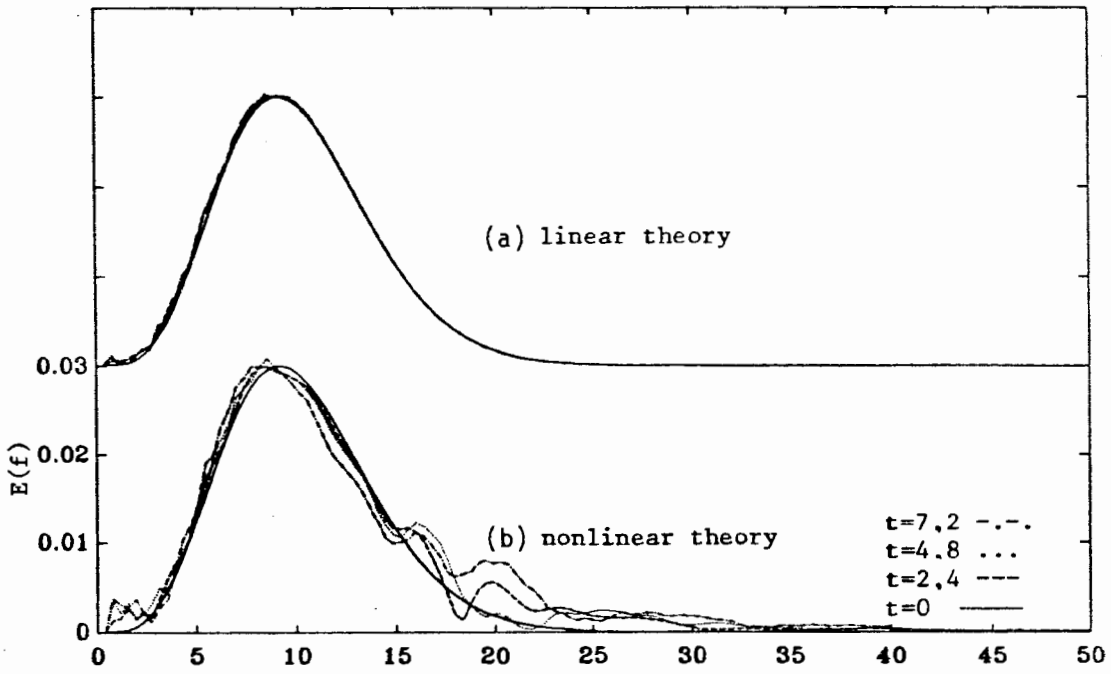

FIG. 5. Nonlinear and linear spectral evolution